Diversified regulation of circadian clock gene expression following whole genome duplication

Alexander C. West[1], Marianne Iversen[1], Even H. Jørgensen[1], Simen R. Sandve[2], David G. Hazlerigg[1], Shona H. Wood[1]*

1 Arctic chronobiology and physiology research group, Department of Arctic and Marine Biology, UiT – The Arctic University of Norway, Tromsø NO-9037, Norway

2 Centre for Integrative Genetics (CIGENE), Department of Animal and Aquacultural Sciences (IHA), Faculty of Life Sciences (BIOVIT), Norwegian University of Life Sciences (NMBU), 5003 Ås, Norway

* Corresponding author shona.wood@uit.no

Keywords: Whole genome duplication, Circadian, Photoperiod, Rediploidization, Anadromy, Smoltification, Cortisol, Atlantic salmon, *Salmo salar*.

Short title: Circadian clock gene regulation and whole genome duplication

Abstract

Across taxa, circadian control of physiology and behavior arises from cell-autonomous oscillations in gene expression, governed by a networks of so-called 'clock genes', collectively forming transcription-translation feedback loops. In modern vertebrates, these networks contain multiple copies of clock gene family members, which arose through whole genome duplication (WGD) events during evolutionary history. It remains unclear to what extent multiple copies of clock gene family members are functionally redundant or have allowed for functional diversification. We addressed this problem through an analysis of clock gene expression in the Atlantic salmon, a representative of the salmonids, a group which has undergone at least 4 rounds of WGD since the base of the vertebrate lineage, giving an unusually large complement of clock genes. By comparing expression patterns across multiple tissues, and during development, we present evidence for gene- and tissue-specific divergence in expression patterns, consistent with functional diversification of clock gene duplicates. In contrast to mammals, we found no evidence for coupling between cortisol and circadian gene expression, but cortisol mediated non-circadian regulated expression of a subset of clock genes in the salmon gill was evident. This regulation is linked to changes in gill function necessary for the transition from fresh- to sea-water in anadromous fish. Overall, this analysis emphasises the potential for a richly diversified clock gene network to serve a mixture of circadian and non-circadian functions in vertebrate groups with complex genomes.

Author Summary

The generation of daily (circadian) rhythms in behaviour and physiology depends on the activities of networks of so-called clock genes. In vertebrates, these have become highly complex due to a process known as whole genome duplication, which has occurred repeatedly during evolutionary history, giving rise to additional copies of key elements of the clock gene network. It remains unclear whether this results in functional redundancy, or whether it has permitted new roles for clock genes to emerge. Here, based on studies in the Atlantic salmon, a species with an unusually large complement of clock genes, we present evidence in favour of the latter scenario. We observe marked tissue-specific, and developmentally-dependent differences in the expression patterns of duplicated copies of key clock genes, and we identify a subset of clock genes whose expression is associated with the physiological preparation to migrate to sea, but is independent of circadian regulation. Associated with this, cortisol secretion is uncoupled from circadian organisation, contrasting with the situation in mammals. Our results indicate that whole genome duplication has permitted clock genes to diversify into non-circadian functions, and raise interesting questions about the ubiquity of mammal-like coupling between circadian and endocrine function.

51 **Introduction**

52 Circadian control of metabolic physiology and behaviour is a ubiquitous characteristic across
53 taxa [1–3]. In eukaryotes, circadian control derives from a cell-autonomous molecular
54 oscillator, assembled from a regulatory network of transcription factors, co-factors, (co-)
55 regulators, chromatin modifiers and an array of post-translational regulators of protein
56 function, often described collectively as 'clock genes' [1]. Clock gene oscillations coordinate
57 the transcription of multiple genes to exert effects on global cell metabolism [1]. While the
58 molecular clock is conserved between insects and mammals [2], the mammalian network
59 contains many duplicated components as a consequence of both local and whole genome
60 duplication (WGD).

61 Two rounds of WGD preceded the establishment of the tetrapod lineage 500 million
62 years ago (MYA) (Figure 1A), and gave rise to the complement of clock genes seen in
63 mammals, including multiple paralogues of *Period* and *Cryptochrome* genes. Paralogues
64 arising from WGD are known as 'ohnologues', after Susumu Ohno, who wrote a seminal
65 monograph hypothesising that the genetic redundancy proceeding WGD facilitates
66 evolutionary innovation [4,5]. Nevertheless, the evolutionary importance and extent to
67 which clock gene ohnologues are functionally divergent largely remains unclear [6–10].
68 Indeed the retention of multiple redundant ohnologues of core clock genes is puzzling given
69 that the essential role of the circadian clock has not changed during the course of
70 evolutionary history [1,2,11,12]. Conceivably, functional differences between ohnologues,
71 achieved either by coding sequence differences or by promoter-based differences in
72 expression level, could enable tissue-specific optimization of function, but evidence for this
73 is sparse [11,12]. It has been suggested that preferential interactions of ancient duplicated

74 mammalian PERIOD proteins with specific duplicated mammalian CRYPTOCHROME proteins
75 may affect photic entrainment [13], but experimental evidence is lacking [14]. Tissue-specific
76 functions of mammalian CKIδ/ε ohnologues in regulation of PERIOD protein stability have
77 been suggested [15], and alterations in period (tau), amplitude and clock resetting behavior
78 have been observed but clear distinctions of function between the ohnologues are lacking
79 [8,16–18].

80 Following the two basal vertebrate WGD events (Figure 1A), subsequent rounds of
81 WGD have occurred in several linages, resulting in highly complex genomes containing
82 thousands of ohnologue pairs. This is exemplified by the situation found in the salmonids,
83 which underwent two additional rounds of WGD compared to basal vertebrates; a third
84 WGD (Ts3R) shared by all teleost fish, and a more recent, the salmonid-specific fourth round
85 of duplication (Ss4R) taking place some 100 MYA (Figure 1A) [19]. The Ss4R event is a
86 defining characteristic of the salmonid group and is theorized to have led to the evolution of
87 anadromy; an adaptation of freshwater salmonids to spend part of their life-cycle at sea
88 [20]. Genome-scale analysis in salmonids has begun to provide new insights into the
89 evolutionary significance of ohnologue divergence [21,22]. Impressively, even though gene
90 loss often occurs following duplication events (reviewed in:[23]), there remains a rich
91 complexity of clock genes in teleosts compared to mammals. Of the 18 clock genes (as
92 defined in Figure 1B) identified in laboratory mice the zebrafish genome contains 30, and the
93 Atlantic salmon genome contains 61 clock genes (S1 Table, S1 appendix).

94 To understand why so many additional copies of core clock genes are retained, we
95 have undertaken a comprehensive analysis of clock gene expression in the Atlantic salmon,
96 exploring temporal regulation in different tissues and responsiveness to different

97 environmental stimuli. Here, we show diversified regulation of clock ohnologues as a result
98 of WGD, reflecting the fundamental differences in temporal organization of metabolism
99 between tissues.

100 **Results**

101 **Tissue-specific expression of clock gene ohnologues indicates regulatory divergence**

102 To identify all conserved clock genes in the Atlantic salmon we extracted amino acid
103 sequences from the well-characterized mouse clock gene network (Figure 1B) then searched
104 for homologous sequences in Atlantic salmon [22] and 12 other vertebrates (S1 appendix,
105 Materials and Methods, *Evolutionary analysis*). Homology relationships between protein
106 sequences were traced back to the root of the vertebrate tree, revealing 61 canonical clock
107 genes in the Atlantic salmon. Comparing the repertoire of clock genes in spotted gar (2
108 WGDs), zebrafish (3 WGDs), and Atlantic salmon (4 WGDs) (Figure 1A) we find no difference
109 in gene retention for loop 1 versus loop 2 genes (Figure 1B). Forty-two of the 61 salmon
110 circadian genes are duplicates arising from the salmonid specific genome duplication and
111 can be assigned to 21 Ss4R specific ohnologue pairings (referred to as Ss4R pairs from here
112 on), while for the remaining 19 genes no extant Ss4R duplicate can be identified suggesting
113 gene loss after WGD (S1 Table, S1 appendix). The chromosomal locations of the Ss4R pairs
114 are shown on Figure 1C, and for ease of comparison the genes will be referred to by their
115 gene name and chromosome. The S1 Table lists the specific gene identifiers and orthologues
116 to zebrafish, medaka, spotted gar and mouse.

117 Following an autopolyploidization, such as the Ss4R, the tetraploid genome will
118 accumulate mutations which block recombination and thereby accelerates duplicate
119 divergence (referred to as rediploidization) [24]. This process has occurred at different rates
120 in different genomic regions in salmonids. Using published data [22] on sequence similarity
121 in 1Mbp windows across syntenic Ss4R regions we could classify the rediploidization times
122 for our 21 Ss4R pairs from early (approx. 87% sequence similarity) to late (>95% sequence

123 similarity)(Figure 1C) and assess whether the history of rediploidization was associated with
124 regulatory divergence.

125 RNA profiling from 13 different tissues [22] demonstrated tissue-specificity of clock
126 gene expression, and particularly highlighted the wide variety and high abundance of clock
127 genes in the brain (S1 Figure). To assess the divergence between Ss4R pairs we calculated an
128 expression divergence index (EDI), based on the relative expression of each member of a
129 pair across all tissues expressed as a ratio (Figure 1D). This revealed evidence for divergent
130 tissue-specific expression within multiple Ss4R pairs but no clear relationship to approximate
131 time of rediploidization (Figure 1D). The Cry3-Ch12/Ch22 pair had the highest EDI, largely
132 attributable to divergent expression in the brain and gill (S1 Figure). The three Ss4R pairs of
133 *Nr1d1* (*Rev-erbα*) and *Nr1d2* (*Rev-erbβ*), which encode transcriptional repressors linking the
134 circadian clock to energy metabolism [25], were also highly divergently expressed genes,
135 again due to differences in the brain and gill (Figure 1D, S1 Figure). Hence tissue-specific
136 expression divergence is a feature of particular aspects of the circadian clockwork.

137

138 **Circadian and light-regulated Ss4R pair expression differs between tissues but is highly**
139 **similar within tissues**

140 To test for circadian regulation of gene expression we collected samples from fish kept in a
141 light dark cycle (diel), constant light (LL) and constant dark (DD) (Figure 2A, see Circadian
142 experiment I, Materials and Methods). To avoid unintended rhythmical stimuli (zeitgebers),
143 fish were fasted from 48 hours before the first sampling point and temperature was held
144 constant. We focussed on three tissues with distinctive roles in salmonid physiology: the
145 optic tectum (OT) of the brain, because it is linked to visual processing and is coupled

146 directly and indirectly to light input [26–29]; the saccus vasculous (SV) because it has been
147 proposed as a mediator of photoperiodic responses [30]; and the gill because it is essential
148 for respiratory gas exchange, ion- and water balance [31]. We hypothesized that expression
149 profiles of clock genes in these three tissues would differ reflecting tissue-specific
150 differences in temporal metabolic demand. We analysed RNA transcript profiles using a
151 bespoke NanoString CodeSet which could specifically identify 46 clock gene targets including
152 17 Ss4R pairs (S2 Table, S2A Figure & S2 appendix).

153 In diel conditions, we identified 28 oscillating transcripts (JTK-cycle adj.p<0.05, S1
154 Table) [32] (Figure 2B). Of the three tissues studied, the OT showed by far the strongest
155 oscillations in gene expression, both under diel and constant conditions (Figure 2B & C). For
156 half of the genes identified, oscillation was only observed in the OT, and even for genes
157 showing significant oscillation across tissues (e.g. Per1-Ch4) the amplitude of oscillation was
158 clearly highest in the OT (Figure 2B & D).

159 In contrast, rhythmicity in both the SV and gill was much less robust. In the SV, only
160 Nr1d1-Ch6 maintained rhythmicity and phase under DD, while in the gill only Arntl1-Ch10
161 maintained rhythmicity and phase under DD (S2B-C Figure). Hence robust circadian
162 rhythmicity is a feature of the salmon brain, but gene expression rhythms are severely
163 dampened in the peripheral tissues we studied.

164 Although differences in absolute expression levels were widely seen within Ss4R pairs
165 - both across and within tissues, when comparing temporal dynamics of expression, within a
166 given tissue they were typically similar (Figure 2D, S1 Table, S2 appendix). This is exemplified
167 by the almost superimposable expression patterns seen for the Per1-Ch4/11 pair (Figure 2D),
168 and for the Tef-Ch3/6 pair (Figure 2D). Indeed, only two significant within-pair differences in

169 expression profile were observed (non-linear regression p-value <0.01, S1 Table, S2D-E
170 Figure): the Arntl1-Ch10/16 pair, with Arntl1-Ch10 showing more robust and higher
171 amplitude rhythmicity than Arntl1-Ch16 in the OT (Figure 2D & S2D-E Figure), and the
172 arrhythmic Cry3-Ch12/22 pair, with Cry3-Ch22 showing a light-induced increase in
173 expression following transfer to LL in the SV (Figure 2D & S2E Figure). Interestingly, we do
174 not observe light responses through Tef as reported in zebrafish [33].

175

176 **Regulatory divergence of clock gene ohnologues within a tissue during a developmental**
177 **transition**

178 The lack of circadian regulatory divergence among Ss4R pairs led us to consider whether
179 retention of duplicates might be related to developmental changes in tissue function. One
180 striking example of this in salmon is the transformation of gills during smoltification from a
181 salt retaining, water excreting organ in freshwater to a salt excreting water retaining organ
182 in seawater [34]. This developmental transition during the anadromous lifecycle relies on
183 hormonally-driven changes in physiology, dependent on seasonally changing day-length
184 (photoperiod) [34]. We therefore performed a photoperiod manipulation experiment, over
185 110 days, to assess the impact of photoperiod-dependent developmental changes in juvenile
186 salmon (parr) (Figure 3A, see smoltification experiment, Materials and Methods). This
187 protocol produces a seawater-tolerant (smolt) phenotype within 4-6 weeks of return to LL
188 (S3 Figure) (reviewed in:[34]).

189 We identified 30 clock genes showing significant changes in expression over the 110
190 days of the experiment (FDR<0.01, S1 Table, Figure 3B); 3 clock genes were undetectable by
191 RNAseq, while a further 28 were present but did not change significantly over time. Amongst

192 the differentially regulated genes we found 9 Ss4R pairs (18 genes) where both copies within
193 a pair showed smoltification-associated regulation, while for 3 pairs only one copy of the
194 pair showed significant changes in expression during smoltification.

195 Gene expression correlation cluster analysis of the differentially expressed genes
196 revealed 5 distinct patterns of expression over the experiment indicating that different
197 regulatory pathways are directing the expression of particular clock genes during
198 smoltification (Figure 3B). Based upon this analysis we identified 6 Ss4R pairs within which
199 evidence of developmental regulatory divergence could be observed (Figure 3C). For 3 of
200 these Ss4R pairs only one member showed a developmental change in expression (Figure 3C,
201 Cry3-Ch12/22, Rora-Ch2/5, Rora-Ch10/16) , while for the 3 remaining Ss4R pairs the
202 dynamics of expression, as defined by cluster analysis, differed within the pairing (Figure 3C,
203 Nr1d2-Ch2/5, Per1a-Ch4/11, CKIδ-Ch1/28). Therefore we see strong developmental
204 regulation of clock genes in the gill over 110 days, contrasting with the lack of circadian
205 regulation.

206

207 **Glucocorticoid signaling induces clock ohnologue expression and accounts for regulatory**
208 **divergence observed in the Ss4R pair Tef-Ch3/6**

209 While glucocorticoids play a major role in the circadian organization of mammals (reviewed
210 in: [35]), the evidence for an analogous role in fish is unclear (References summarized in: S3
211 Table). Nevertheless, cortisol is a major hormonal regulator of smoltification in Atlantic
212 salmon, steadily rising during this photoperiod-driven seasonal process [36]. We collected
213 blood samples from fish kept in a light dark cycle (LD - 6:18) and in constant conditions (LL or
214 DD) and found no evidence of diel or circadian rhythmicity in cortisol secretion (Figure 4A,

215 see Circadian experiment II, Materials and Methods, S4 Table) along with weak or absent
216 peripheral tissue clock gene circadian oscillation (S2B-C Figure). We hypothesized that the
217 changes in gene expression observed in Figure 3 may be due to seasonally increasing cortisol
218 during smoltification, therefore if we induced cortisol through a simple stress test we may
219 induce the same clock genes seen during smoltification.

220 To test this we conducted a 24 hour seawater (SW) challenge test in freshwater-
221 adapted fish (Figure 4B, see Smoltification experiment, Materials and Methods) eliciting an
222 osmotic stress-mediated increase in cortisol secretion (Figure 4C). Gills were collected from
223 SW and fresh water (FW) groups. We identified 15 clock genes showing significant changes
224 in expression in response to SW by RNAseq (FDR<0.01, S1 Table, Figure 4D). Importantly,
225 87% of acutely SW-responsive clock genes (13/15) also change over the chronic
226 developmental time-scales of smoltification (Figure 3, S1 Table). Amongst the SW responsive
227 genes we found 3 Ss4R pairs (6 genes) where both copies responded to SW, and 6 pairs
228 where only one of the pair changed expression in SW. To assess regulatory divergence within
229 these 9 pairs we plotted the fold change in response to SW for and determined that 5 of the
230 pairs showed significant regulatory divergence (two-way ANOVA <0.01, S1 Table, Figure 4E).

231 To further examine if glucocorticoid signaling, via cortisol, was responsible for the
232 induction of clock genes in the gill we used transcription factor binding site analysis [37] on
233 clock genes induced by SW (15 genes) compared to 43 clock genes that were SW-insensitive.
234 SW-induced circadian genes promoters were highly enriched for HSF1 (heat shock factor 1),
235 FOXO1 (forkhead box O1), MAX1 (myc-assocated factor X1) and glucocorticoid receptor
236 response elements (GR) (Figure 4F, S5 Table). Smoltification and responses to SW-exposure
237 are coordinated by multiple endocrine factors including cortisol, growth hormone (GH) and

238 IGF-1 [38,39]. HSF-1 and FOXO-1 elements are regulated by IGF1 signaling, during stress,
239 cellular metabolism and development [40–44]. Furthermore, the enrichment of GR
240 implicates non-circadian glucocorticoid signaling in the induction of clock genes in the gill
241 during smoltification and stress.

242 Next we wanted to experimentally test the *in-silico* association with glucocorticoid
243 signaling and ask whether differential sensitivity to glucocorticoid signaling might account
244 for the differential regulation observed within Ss4R pairs. We treated isolated gill arches
245 with dexamethasone (DEX; a GR agonist) for 24h and then measured the gene expression of
246 the 5 Ss4R pairs using qPCR (Figure 5A, S6 Table). We validated the experiment by
247 assessment of a positive control gene: *Tsc22d3* (*Gilz*) [45](S4 Figure). We found that whilst
248 some of the genes are glucocorticoid sensitive (3/10), supporting the *in-silico* association,
249 the majority are not induced by glucocorticoids (Figure 5B-D). However, we do demonstrate
250 divergence in the regulation of the Tef-Ch3/6 pair in response to glucocorticoids (Figure 5D).

251 **Discussion**

252 Divergent regulation of gene expression is a major contributor to the evolution of novel
253 adaptations and species diversity [46,47]. Our analysis of the circadian clock network in the
254 Atlantic salmon reveals clear evidence of diversified expression regulation among the many
255 retained copies of canonical clock genes that have arisen through successive WGD events.
256 Diversified regulation is seen in tissue-specific expression patterns (Figure 1), and in
257 response to developmental and environmental stimuli (Figures 3, 4, 5). Ultimately, these
258 differences likely reflect the uneven influence of diel factors on metabolism and cellular
259 processes in central and peripheral tissues in a cold blooded fish. Altered sensitivity to GR-
260 signalling, likely mediated through the cortisol axis, emerges as one proximate cause of
261 differences in tissue-specific expression dynamics (Figures 4, 5). Overall this analysis
262 emphasises the potential for a richly diversified clock gene network to serve non-circadian
263 functions in vertebrate groups with complex genomes.

264 A striking contrast emerges between clock gene expression regulation in the OT and
265 the gill. The OT is a brain site which is coupled to light input both through retinal afferents,
266 photoreceptor expression, and indirect melatonin-mediated input via OT melatonin
267 receptors [26–29]. In contrast, the gill is directly exposed to the water environment and
268 continuously handles the osmotic and energetic challenges that this presents [48–50]. Thus
269 while both tissues are highly metabolically active and heavily reliant on ATPase activity to
270 maintain function, the principal environmental influence for the OT is rhythmic light dark
271 input, while for the gill it is continuous osmotic challenge.

272 Given these differences in tissue function, it is not surprising to observe different
273 complements of clock genes in the two tissues and dramatic differences in temporal

274 dynamics (Figure 2). In the diel-sensitive OT a dominant diel / circadian influence on
275 expression is seen, while in the gill this is a much weaker influence. Nonetheless, clock gene
276 expression in the gill is dynamically regulated, both over the chronic developmental time-
277 scales of smoltification, and acutely in response to osmotic stress. The finding that the
278 complement of genes showing highly sensitive changes in expression in the gill is largely
279 non-overlapping with that under light / circadian control in the OT is clear evidence for
280 diverged expression regulation within the circadian network.

281 Previous work has identified several Atlantic salmon clock genes that cycle in diel
282 conditions [51–53]. While confirming these earlier findings, our analysis goes far beyond
283 them by showing how the entire clock network is regulated under diel and constant
284 conditions in serval tissues. We show that only the OT shows persistent rhythmicity under
285 constant conditions, not the SV or gill (Figure 2). These results sit in contrast to the zebrafish
286 circadian system in which tissue autonomous clock gene oscillation are seen in all tissues
287 investigated [54]. Specific elements of the zebrafish clock appear to be fundamentally
288 different to the Atlantic salmon clock. For example zebrafish Cry1a is acutely light-induced
289 and appears to pause the circadian mechanism under LL [9], whereas the closest salmon
290 orthologues to zebrafish Cry1a, Cry1-Ch10 and Cry1-Ch16, are not light-induced and show
291 persistent rhythmicity in the OT under LL (S1 Table). Instead the salmon orthologues to
292 zebrafish Cry3b, Cry3-Ch22 and Cry3-Ch12, are acutely induced by light and salt,
293 respectively. Light induction of Zebrafish Tefa [33] is not seen in the closest salmon
294 orthologues Tef-Ch1 and Tef-Ch28, however, the zebrafish Tefb orthologues, Tef-Ch3 and
295 Tef-Ch6 are seawater induced. In zebrafish, Tef transcription is induced in response to light
296 and UV exposure producing reactive oxygen species (ROS) which act on the D-box in the Tef
297 promoter, initiating a DNA damage repair cascade [55]. Importantly this light-mediated ROS

298 inducibility of Tef appears to be absent in cave fish and mammals [55], suggesting a
299 zebrafish-specific adaptation to UV light exposure, potentially related to spawning
300 environment [56]. In our study we found no enrichment for genes associated with oxidative
301 stress in either the seawater challenge or photoperiodic treatment groups but the
302 photoperiod-driven smoltification induction of all four Tef genes is noteworthy, as is the
303 seawater specific induction of the Ss4r pair Tef-Ch3 and Ch6, and the apparent regulatory
304 divergence of these duplicates in glucocorticoid responsiveness. These species differences
305 indicate plasticity of the circadian clock in response to different environmental stressors
306 depending on life history.

307 Within the Atlantic salmon the distinct tissue-specific expression dynamics we
308 observe and the smoltification and stress-related induction of clock genes focuses attention
309 on cortisol [34,35,57]. In mammals cortisol is a major player in circadian organization, acting
310 as an internal zeitgeber through which the hypothalamic–pituitary–adrenal (HPA) axis can
311 coordinate daily changes in tissue activity throughout the organism (reviewed in: [35]).
312 Because the teleost hypothalamic–pituitary–interrenal (HPI) axis is functionally analogous to
313 the HPA axis [57], there has been a widespread assumption that cortisol plays a similar
314 circadian coordination function in teleosts [58], although definitive evidence for this is
315 lacking (S3 Table)[59]. Indeed our study implies that it is unlikely that cortisol plays a
316 circadian role in salmonids – we found no evidence for circadian or even diel changes in
317 cortisol secretion in Atlantic salmon (Figure 4A), and GREs are less enriched in circadian
318 oscillating clock genes than in non-oscillating, development- and SW-sensitive clock genes
319 (Figure 4F). Hence while our data strongly implicate cortisol in the dynamic expression of a
320 subset of Atlantic salmon clock genes, this seems to have nothing to do with circadian
321 function *per se*, and more to do with a role for these genes in non-circadian influences of the

322 HPI axis. It is interesting to speculate that this shifting relationship between glucocorticoids
323 and clock genes could be a contributory factor for the evolution of anadromy and the
324 regulation of its seasonal timing. Furthermore, this finding raises interesting questions about
325 the ubiquity and evolutionary origins of mammal-like coupling between the HPA axis and
326 circadian function.

327 While evidence of functional divergence in ancient duplicated cryptochromes, and,
328 sequence divergence of Ts3R cryptochromes in zebrafish have been observed [60] we
329 expected that Ss4R generated significant genetic complexity in the salmonid circadian clock
330 and therefore asked how expression patterns diverged within Ss4R pairs. Intriguingly, the
331 answer to this question was highly dependent upon context. We saw many examples of
332 pronounced within-Ss4R pair differences in terms of tissue-specific expression, and some
333 50% of identifiable Ss4R pairs showed within-pair divergence in expression during
334 smoltification. But within-pair divergence in daily expression patterns was hardly observed.
335 Why might this be so? We suggest this may reflect a difference in the way that selection
336 pressures have operated on promoter regions to, on the one hand modulate tissue-specific
337 expression and, on the other daily temporal regulation. According to this view duplication
338 would confer freedom to diverge, thereby meeting differing tissue-specific requirements.
339 Conversely, the daily temporal patterning may be so fundamental to cell function that any
340 mutations leading to deviation from the ancestral dynamics were strongly selected against.
341 This conjecture will require detailed analysis of regions of promoter conservation /
342 divergence among Ss4R pairs.

343 **Materials and Methods:**

344 *Evolutionary analysis*

345 To identify gene orthologs and ohnologs we generated protein sequence homology based
346 orthogroups using the Orthofinder pipeline [61]. For each orthogroup we used the resulting
347 protein tree topology to manually annotate pairs of salmon ohnologs based on the following
348 criteria: (i) salmon ohnologs should form a monophyletic clade only containing genes from
349 other salmonid species, (ii) this monophyletic salmonid clade must have Northern pike as the
350 sister group, and (iii) putative ohnolog pairs had to be conserved in minimum one other
351 salmonid species. Finally, we only retained putative ohnolog if their genomic positions were
352 defined as syntenic regions originating from the Ss4R as defined in Lien *et al.* [22]. Maximum
353 likelihood gene trees with bootstrap values for all genes included in the study are presented
354 in S1 appendix. These trees include the following species: human, mouse, spotted gar,
355 zebrafish, stickleback, medaka, northern pike, grayling, danube salmon, arctic charr, coho
356 salmon, rainbow trout, Atlantic salmon. The relevant scripts, input files and resulting trees
357 are also available here. For quick reference S1 table presents the salmon gene loci and their
358 corresponding orthologues in Zebrafish, spotted gar, medaka and mouse.

359 *Multi-tissue analysis*

360 Publically available data was used to assess the multi-tissue expression in the Atlantic
361 salmon (one adult male, kept in freshwater), these data can be found in the NCBI Sequence
362 Read Archive (SRA): PRJNA72713 and PRJNA260929.

363 *Ethics statement*

364 Fish handling and euthanasia was performed by competent persons and in accordance with
365 the European Union Regulations concerning the protection and welfare of experimental
366 animals (European directive 91/492/CCE). The experiment was approved by the Norwegian
367 Committee on Ethics in Animal Experimentation (ID 3630).

368 *Animal husbandry*

369 Juvenile Atlantic salmon (*Salmo salar*, Linnaeus, 1758) of the Aquagene commercial strand
370 (Trondheim, Norway) were used in all experiments. Fish were held under constant light (LL;
371 >200 lux), at 10° from hatching onwards, and kept in 500 L tanks from first feeding. The fish
372 were approximately 7 months old when the experiments were initiated. Up until that time
373 the fish had been feed continuously with pelleted salmon feed (Skretting, Stavanger,
374 Norway), from automatic feeders.

375 *Circadian experiment I*

376 Fish were maintained in 500L freshwater were transferred from LL to a short photoperiod
377 (SP; 6L:18D) light schedule for 8 weeks before the start of the experiment. Short
378 photoperiods provide a strong zeitgeber (timing signal) entraining the fish to a light dark
379 cycle. In order to test for a circadian rhythm it is necessary to remove any zeitgebers, light,
380 temperature and food are all potential zeitgebers which we controlled for. Two weeks
381 before sampling, fish were distributed to two separate 150L tanks and water temperature
382 was maintained at 14°C (±0.5). Fish were fasted for 48 hours prior to the experiment and
383 throughout the sampling. To identify genes which were driven by an endogenous circadian
384 rhythm we sampled under diel (SP; 6L:18D), constant light (LL) and constant dark conditions
385 (DD). Sampling was at 4 hour resolution starting at ZT5 (zeitgeber time; time since lights on)
386 in diel conditions (n= 3 per time point, 7 time-points), transitioning onto either LL or DD. In

387 LL sampling was from CT9 (circadian time) at a 4 hour resolution (n = 3 per time-point, 6
388 time-points) because ZT 1 and 5 in this design can also be defined as CT1 and 5. In DD
389 samples were collected from CT1 at a 4 hour resolution (n = 3 per timepoint, 8 time-points)
390 (Figure 2A). For the statistical analysis ZT5 to ZT5 was used for diel conditions, and CT9 to
391 CT29 for constant conditions. Collections during the dark phase were conducted under dim
392 red light. During sampling fish were netted out and euthanized by an overdose of
393 benzocaine (150ppm). Weight and length were recorded and no significant variation noted.
394 Optic tectum, gill and saccus vasculous were dissected and snap frozen on dry ice. RNA was
395 extracted for subsequent nanostring profiling.

396 *Circadian experiment II*

397 Fish were maintained in 500L freshwater were transferred from LL to a short photoperiod
398 (SP; 6L:18D) light schedule for 20 weeks before the start of the experiment. Two weeks
399 before sampling, fish were distributed to two separate 150L tanks. Fish were fasted for 48
400 hours prior to the experiment and throughout the sampling. Temperature was maintained at
401 an average of 8.5°C ±1. Sampling was at a 4 hour resolution starting one hour after lights on
402 (ZT1), maintaining the fish under diel conditions (SP; 6L:18D) for 24 hours and then switching
403 to either LL or DD, and sampling at 4h resolution for a further 29 hours (n = 4 per time-point)
404 (Figure 4A). Collections during the dark phase were conducted under dim red light. During
405 sampling fish were netted out and euthanized by an overdose of benzocaine (150ppm).
406 Weight and length were recorded and no significant variation noted. Blood was collected at
407 each time-point from the caudal vein in heparinized vacutainers. Blood samples were
408 centrifuged at 500 x g for 15 min to collect plasma for subsequent hormone analysis.

409 *Smoltification experiment and seawater tests*

410 Using a standard aquaculture and research method we used photoperiod to induce the
411 developmental transition of juvenile salmon (parr) to seawater prepared fish (smolts). This
412 method requires switching parr on constant light to short photoperiod (SP; 6L:18D) for at
413 least 8 weeks before returning the fish to constant light where over 4 weeks they gain osmo-
414 regulatory capacity in seawater (Figure 3A). Fish were maintained in 150L freshwater tanks
415 at an average 8.5°C ±1 and were transferred from LL to SP (8L:16:D) for 8 weeks before
416 return to LL for 7 weeks. Fish were sampled at six time-points in fresh-water shown in Figure
417 3A (T1-T6, n = 6 per time-point), these time-points are designed to capture the
418 photoperiodically induced transition from parr to smolt. Fish were fasted for 48 hours prior
419 to sampling. Gills were collected into RNAlater (Sigma-Aldrich, St. Louis, Missouri, USA),
420 storing at 4°C for 24 hours, before being transferred to -80°C. RNA was extracted and used
421 for RNA-seq (Data shown in Figure 3).

422 To validate the photoperiod protocol seawater challenge tests were conducted on a
423 randomly selected subgroup that were transferred to a 100L tank supplied with seawater
424 (34% salinity) for 24 hours. Fish were netted out after 24 hours and euthanized by an
425 overdose of benzocaine (150ppm). Blood samples were collected from the caudal vein in
426 heparinized vacutainers and plasma was collected and stored at -20□. To test the osmolality
427 of blood thawed plasma samples were analysed for osmolyte content using a Fiske One-Ten
428 Osmometer (Fiske Associates, Massachusetts, USA, ± 4 mOsm kg-1). These tests were
429 conducted from T2 to T6 (n = 12 per time-point), and confirm that from T5 (29 days after the
430 return to LL) the fish had osmo-regulatory capacity in seawater (S3 Figure). Gills were
431 collected at each time-point after seawater challenge (n= 6 per time-point), RNA was
432 extracted and RNA-seq preformed as above. All data are available from the European
433 nucleotide archive under project number: PRJEB34224. This study presents data from the

434 freshwater groups at all time-points (Figure 3) and seawater challenged fish at T4 only
435 (Figure 4B). T4 is 8 days after return to LL and therefore these fish do not have osmo-
436 regualtory capacity in seawater and are used as a stress test comparison to fish from the
437 same time-point kept in freshwater (Figure 4B – F).

438 *In-vitro Gill Culture*

439 Juvenile Atlantic Salmon were prepared as in the smoltification experiment, sampling at the
440 equivalent of T4 (8 days after return to LL) (Figure 5A). Following euthanasia whole gill
441 arches were rapidly dissected (biological replicates, n=4 per treatment), excess mucus was
442 removed by careful blotting onto tissue paper before the arches were transferred
443 individually into 50 ml of pre-prepared control or treatment media. The prepared media
444 consisted of Leibovitz L-15 (Lonza) supplemented with non-essential amino acids (1%, 100x
445 Lonza), sodium-pyruvate (1%, 100x Lonza), 0.05 mg/ml gentamycin (Sigma) and 20% fetal
446 bovine serum (FBS, sigma). The experimental group was supplemented with 0.1M
447 dexamethasone diluted in DMSO (dimethyl-sulphoxide, Sigma) to a final concentration of
448 0.1µM. The control group contained an equivalent concentration of DMSO (0.1%). The
449 excised gill arches were incubated for 24h at 4°C, gill filaments were removed with a scalpel
450 and snap frozen on dry ice before being stored at -80°C. RNA was extracted for qPCR
451 analysis.

452 *RNA extraction*

453 RNA extraction for RNAseq was performed using a TRIzol-based method (Invitrogen, Thermo
454 Fisher, Waltham, Massachusetts, USA), and in accordance with the manufacturers
455 recommendation. Resulting RNA concentrations and quality were checked using a NanoDrop

456 spectrophotometer (NanoDrop Technologies, Wilmington, DE, USA). RNA was stored at -
457 80°C.

458 For nanostring and qPCR, SVs were extracted using QIAgen RNeasy micro kit, OT and gill
459 tissues were extracted using QIAgen RNeasy mini kit according to the manufacturers
460 instructions. RNA concentration was quantified and quality confirmed using the Experion
461 Automated Electrophoresis System (BioRad).

462 *Nanostring*

463 Custom nanostring codesets were designed by Nanostring Technologies Inc. using the
464 Atlantic Salmon reference genome (Cigene), accession numbers and target sequences are
465 shown in S2 Table. Codesets were processed by the Univerisity of Manchester Genomic
466 Technologies Core Facility. This technology is based on the use of fluorescent barcoded
467 probes which bind specifically to the target molecule. Importantly these barcodes should
468 only bind one at a time to each target molecule, therefore the number of fluorescent
469 barcodes reflects the number of RNA molecules of your target gene. A spike control with a
470 known number of RNA molecules was also used to normalise across samples and runs.
471 Therefore the units are counts normalised to spike-in positive controls. Data was processed
472 using nSolver 4.0 software (Nanostring). Data can be accessed on GEO under the project
473 identifier GSE146530.

474 *Transcriptome sequencing and assembly*

475 Libraries were prepared using TruSeq Stranded mRNA HS kit (Illumina, San Diego, California,
476 USA). Mean library length was determined using the 2100 Bioanalyzer with the DNA 1000 kit
477 (Agilent Technologies, Santa Clara, California, USA). Library concentrations was determined
478 using the Qubit BR kit (Thermo Scientific, Waltham, Massachusetts, USA). Samples were

479 barcoded with Illumina unique indexes. The Illumina HiSeq 2500 was used to perform single-
480 end 100-bp sequencing of samples at the Norwegian Sequencing Centre (University of Oslo,
481 Oslo, Norway).

482 Cutadapt (ver. 1.8.1) was used for removal of sequencing adapters and trimming of low
483 quality bases (parameters –q 20, -O 8 -minimum-length 40). Quality control was performed
484 with FastQC software. Reads were mapped onto the references genome using STAR
485 software (ver. 2.4.2a). Read counts for annotated genes were generated using the HTSEQ-
486 count software (ver. 0.6.1p1).

487 All RNAseq data for the smoltification experiment is available in the European nucleotide
488 archive under project number: PRJEB34224.

489 *Analysis of differentially expressed genes*

490 Analysis of differential gene expression was performed with package edgeR (ver. 3.14.0)
491 using R (ver. 3.4.2) and RStudio (ver. 1.0.153). Prior to analysis of differential expression, the
492 raw counts were filtered, setting an expression level threshold of a minimum of one count
493 per million reads (cpm) in five or more libraries, resulting in a list of 33 951 expressed genes.
494 The counts were scaled by applying trimmed means of M-values (TMM) scaling. Exact tests
495 were then performed to find genes that were differentially expressed between FW-kept and
496 24-h SW challenged fish. An ANOVA-like test was performed to find genes that were
497 differentially expressed over T1-T6 FW time-points. The test results were filtered for a false
498 discovery rate (FDR) to be less than 0.01 to identify significantly differentially expressed
499 genes. Clustering analysis was performed using Pearson correlation.

500 Heatmaps were generated in R using custom scripts for pheatmap. Transcription factor
501 binding site analysis was conducted using SalmotifDB [37].

502 *qPCR*

503 cDNA was synthesised from sample total RNA using High capacity RNA to cDNA kit (Applied
504 Biosystems). qPCR was performed using GoTaq Master Mix (Promega) and a 96 well thermal
505 cycler (Applied Biosystems). Relative gene expression was quantified by the ΔΔCT method
506 using *Ef1a* as reference gene. Primer sequences are listed in S2 Table and source data is in S6
507 Table.

508 *Hormone Assays*

509 Cortisol ELISA assays were performed by Stockgrand (UK). Source data in S4 Table.

510 *Statistical analyses*

511 RNAseq analysis is detailed above. Mean difference comparisons were carried out using
512 Student's t-test (two-sided, unpaired), two-way ANOVA with post hoc tests as appropriate
513 (Graphpad Prism 8.1.2). The expression divergence index (EDI) index was calculated as
514 follows: EDI= abs(log2[Gene1/Gene2)].

515 The R package JTK cycle was used to assess rhythmicity of transcripts under LD and constant
516 light or dark conditions [32]. For statistical comparison of gene expression between
517 ohnologue pairs in the circadian experiment, expression was normalized to group mean then
518 best fit sixth-order centered polynomial curves were generated by non-linear regression
519 analysis and shared characteristics tested with extra sum of squares F test (Graphpad Prism
520 8.0).

521 **References**

522 1. Shi M, Zheng X. Interactions between the circadian clock and metabolism: there are
523 good times and bad times. Acta Biochim Biophys Sin (Shanghai). 2013;45: 61–69.
524 doi:10.1093/abbs/gms110

525 2. Rosbash M. The Implications of Multiple Circadian Clock Origins. Michael Young,
526 editor. PLoS Biol. 2009;7: e1000062. doi:10.1371/journal.pbio.1000062

527 3. Young MW, Kay SA. Time zones: a comparative genetics of circadian clocks. Nat Rev
528 Genet. 2001;2: 702–715. doi:10.1038/35088576

529 4. Taylor JS, Raes J. Duplication and divergence: the evolution of new genes and old
530 ideas. Annu Rev Genet. 2004;38: 615–43.
531 doi:10.1146/annurev.genet.38.072902.092831

532 5. Ohno S. Evolution by Gene Duplication. Berlin, Heidelberg: Springer Berlin Heidelberg;
533 1970. doi:10.1007/978-3-642-86659-3

534 6. Horst GTJ van der, Muijtjens M, Kobayashi K, Takano R, Kanno S, Takao M, et al.
535 Mammalian Cry1 and Cry2 are essential for maintenance of circadian rhythms.
536 Nature. 1999;398: 627–630. doi:10.1038/19323

537 7. Erzberger A, Hampp G, Granada AE, Albrecht U, Herzel H. Genetic redundancy
538 strengthens the circadian clock leading to a narrow entrainment range. J R Soc
539 Interface. 2013;10: 20130221. doi:10.1098/rsif.2013.0221

540 8. Pilorz V, Cunningham PS, Jackson A, West AC, Wager TT, Loudon ASI, et al. A Novel
541 Mechanism Controlling Resetting Speed of the Circadian Clock to Environmental
542 Stimuli. Curr Biol. 2014;24: 766–773. doi:10.1016/j.cub.2014.02.027

543 9. Tamai TK, Young LC, Whitmore D. Light signaling to the zebrafish circadian clock by
544 Cryptochrome 1a. Proc Natl Acad Sci. 2007;104: 14712–14717.
545 doi:10.1073/pnas.0704588104

546 10. Shi S, Hida A, McGuinness OP, Wasserman DH, Yamazaki S, Johnson CH. Circadian
547 Clock Gene Bmal1 Is Not Essential; Functional Replacement with its Paralog, Bmal2.
548 Curr Biol. 2010;20: 316–321. doi:10.1016/j.cub.2009.12.034

549 11. Tauber E, Last KS, Olive PJW, Kyriacou CP. Clock Gene Evolution and Functional
550 Divergence. J Biol Rhythms. 2004;19: 445–458. doi:10.1177/0748730404268775

551 12. Looby P, Loudon ASI. Gene duplication and complex circadian clocks in mammals.
552 Trends Genet. 2005;21: 46–53. doi:10.1016/j.tig.2004.11.012

553 13. Daan S, Albrecht U, Van der Horst GTJ, Illnerová H, Roenneberg T, Wehr TA, et al.
554 Assembling a Clock for All Seasons: Are There M and E Oscillators in the Genes? J Biol
555 Rhythms. 2001;16: 105–116. doi:10.1177/074873001129001809

556 14. Hastings M. Modeling the Molecular Calendar. J Biol Rhythms. 2001;16: 117–123.
557 doi:10.1177/074873001129001818

558 15. Meng Q-J, Logunova L, Maywood ES, Gallego M, Lebiecki J, Brown TM, et al. Setting
559 Clock Speed in Mammals: The CK1 tau Mutation in Mice Accelerates Circadian
560 Pacemakers by Selectively Destabilizing PERIOD Proteins. Neuron. 2008;58: 78–88.
561 doi:10.1016/j.neuron.2008.01.019

562 16. Meng Q-J, Maywood ES, Bechtold DA, Lu W-Q, Li J, Gibbs JE, et al. Entrainment of
563 disrupted circadian behavior through inhibition of casein kinase 1 (CK1) enzymes. Proc
564 Natl Acad Sci. 2010;107: 15240–15245. doi:10.1073/pnas.1005101107

565 17. Lee H, Chen R, Lee Y, Yoo S, Lee C. Essential roles of CKIδ and CKIε in the mammalian
566 circadian clock. Proc Natl Acad Sci. 2009;106: 21359–21364.
567 doi:10.1073/pnas.0906651106

568 18. Etchegaray J-P, Machida KK, Noton E, Constance CM, Dallmann R, Di Napoli MN, et al.
569 Casein Kinase 1 Delta Regulates the Pace of the Mammalian Circadian Clock. Mol Cell
570 Biol. 2009;29: 3853–3866. doi:10.1128/MCB.00338-09

571 19. Macqueen DJ, Johnston IA. A well-constrained estimate for the timing of the salmonid
572 whole genome duplication reveals major decoupling from species diversification. Proc
573 R Soc B Biol Sci. 2014;281: 20132881. doi:10.1098/rspb.2013.2881

574 20. Alexandrou MA, Swartz BA, Matzke NJ, Oakley TH. Molecular Phylogenetics and
575 Evolution Genome duplication and multiple evolutionary origins of complex migratory
576 behavior in Salmonidae. Mol Phylogenet Evol. 2013;69: 514–523.
577 doi:10.1016/j.ympev.2013.07.026

578 21. Robertson FM, Gundappa MK, Grammes F, Hvidsten TR, Redmond AK, Lien S, et al.
579 Lineage-specific rediploidization is a mechanism to explain time-lags between genome
580 duplication and evolutionary diversification. Genome Biol. 2017;18: 111.
581 doi:10.1186/s13059-017-1241-z

582 22. Lien S, Koop BF, Sandve SR, Miller JR, Matthew P, Leong JS, et al. The Atlantic salmon
583 genome provides insights into rediploidization. Nature. 2016;533: 200–205.
584 doi:10.1038/nature17164

585 23. Moriyama Y, Koshiba-takeuchi K. Significance of whole-genome duplications on the
586 emergence of evolutionary novelties. 2018;17: 329–338. doi:10.1093/bfgp/ely007

587 24. Li WH. Rate of gene silencing at duplicate loci: a theoretical study and interpretation
588 of data from tetraploid fishes. Genetics. 1980;95: 237–58. doi:7429144

589 25. Cho H, Zhao X, Hatori M, Yu RT, Barish GD, Lam MT, et al. Regulation of circadian
590 behaviour and metabolism by REV-ERB-α and REV-ERB-β. Nature. 2012;485: 123–127.
591 doi:10.1038/nature11048

592 26. Holmqvist BI, Östholm T, Ekström P. Neuroanatomical analysis of the visual and
593 hypophysiotropic systems in Atlantic salmon (Salmo salar) with emphasis on possible
594 mediators of photoperiodic cues during parr-smolt transformation. Aquaculture.
595 1994;121: 1–12. doi:10.1016/0044-8486(94)90003-5

596 27. Meyer RL. Eye-in-water electrophysiological mapping of goldfish with and without
597 tectal lesions. Exp Neurol. 1977;56: 23–41. doi:10.1016/0014-4886(77)90136-4

598 28. Sandbakken M, Ebbesson L, Stefansson S, Helvik JV. Isolation and characterization of
599 melanopsin photoreceptors of atlantic salmon (Salmo salar). J Comp Neurol.
600 2012;520: 3727–3744. doi:10.1002/cne.23125

601 29. Mazurais D, Brierley I, Anglade I, Drew J, Randall C, Bromage N, et al. Central
602 melatonin receptors in the rainbow trout: Comparative distribution of ligand binding
603 and gene expression. J Comp Neurol. 1999;409: 313–324. doi:10.1002/(SICI)1096-
604 9861(19990628)409:2<313::AID-CNE11>3.0.CO;2-1

605 30. Nakane Y, Ikegami K, Iigo M, Ono H, Takeda K, Takahashi D, et al. The saccus
606 vasculosus of fish is a sensor of seasonal changes in day length. Nat Commun. 2013;4:
607 2108. doi:10.1038/ncomms3108

608 31. Evans DH, Piermarini PM, Choe KP. The Multifunctional Fish Gill: Dominant Site of Gas

609 Exchange, Osmoregulation, Acid-Base Regulation, and Excretion of Nitrogenous
610 Waste. Physiol Rev. 2005;85: 97–177. doi:10.1152/physrev.00050.2003

611 32. Hughes ME, Hogenesch JB, Kornacker K. JTK_CYCLE: An Efficient Nonparametric
612 Algorithm for Detecting Rhythmic Components in Genome-Scale Data Sets. J Biol
613 Rhythms. 2010;25: 372–380. doi:10.1177/0748730410379711

614 33. Vatine G, Vallone D, Appelbaum L, Mracek P, Ben-Moshe Z, Lahiri K, et al. Light Directs
615 Zebrafish period2 Expression via Conserved D and E Boxes. Kramer A, editor. PLoS
616 Biol. 2009;7: e1000223. doi:10.1371/journal.pbio.1000223

617 34. Björnsson BT, Stefansson SO, McCormick SD. Environmental endocrinology of salmon
618 smoltification. Gen Comp Endocrinol. 2011;170: 290–298.
619 doi:10.1016/j.ygcen.2010.07.003

620 35. Dumbell R, Matveeva O, Oster H. Circadian Clocks, Stress, and Immunity. Front
621 Endocrinol (Lausanne). 2016;7. doi:10.3389/fendo.2016.00037

622 36. Langhorne P, Simpson TH. The interrelationship of cortisol, Gill (Na + K) ATPase, and
623 homeostasis during the Parr-Smolt transformation of atlantic salmon (Salmo salar L.).
624 Gen Comp Endocrinol. 1986;61: 203–213. doi:10.1016/0016-6480(86)90198-X

625 37. Mulugeta TD, Nome T, To T-H, Gundappa MK, Macqueen DJ, Våge DI, et al.
626 SalMotifDB: a tool for analyzing putative transcription factor binding sites in salmonid
627 genomes. BMC Genomics. 2019;20: 694. doi:10.1186/s12864-019-6051-0

628 38. McCormick SD. Effects of Growth Hormone and Insulin-like Growth Factor I on Salinity
629 Tolerance and Gill Na+, K+-ATPase in Atlantic Salmon (Salmo salar): Interaction with
630 Cortisol. Gen Comp Endocrinol. 1996;101: 3–11. doi:10.1006/gcen.1996.0002

631 39. McCormick SD. Endocrine Control of Osmoregulation in Teleost Fish. Am Zool.
632 2001;41: 781–794. doi:10.1093/icb/41.4.781

633 40. Accili D, Arden KC. FoxOs at the Crossroads of Cellular Metabolism, Differentiation,
634 and Transformation. Cell. 2004;117: 421–426. doi:10.1016/S0092-8674(04)00452-0

635 41. Barthel A, Schmoll D, Unterman TG. FoxO proteins in insulin action and metabolism.
636 Trends Endocrinol Metab. 2005;16: 183–189. doi:10.1016/j.tem.2005.03.010

637 42. Dong XC, Copps KD, Guo S, Li Y, Kollipara R, DePinho RA, et al. Inactivation of Hepatic
638 Foxo1 by Insulin Signaling Is Required for Adaptive Nutrient Homeostasis and
639 Endocrine Growth Regulation. Cell Metab. 2008;8: 65–76.
640 doi:10.1016/j.cmet.2008.06.006

641 43. Li J, Labbadia J, Morimoto RI. Rethinking HSF1 in Stress, Development, and Organismal
642 Health. Trends Cell Biol. 2017;27: 895–905. doi:10.1016/j.tcb.2017.08.002

643 44. Barna J, Princz A, Kosztelnik M, Hargitai B, Takács-Vellai K, Vellai T. Heat shock factor-1
644 intertwines insulin/IGF-1, TGF-β and cGMP signaling to control development and
645 aging. BMC Dev Biol. 2012;12: 32. doi:10.1186/1471-213X-12-32

646 45. Ronchetti S, Migliorati G, Riccardi C. GILZ as a Mediator of the Anti-Inflammatory
647 Effects of Glucocorticoids. Front Endocrinol (Lausanne). 2015;6.
648 doi:10.3389/fendo.2015.00170

649 46. Carroll SB. Evo-Devo and an Expanding Evolutionary Synthesis: A Genetic Theory of
650 Morphological Evolution. Cell. 2008;134: 25–36. doi:10.1016/j.cell.2008.06.030

651 47. Carroll SB. Endless Forms. Cell. 2000;101: 577–580. doi:10.1016/S0092-
652 8674(00)80868-5

653 48. McCormick SD, Saunders R. Preparatory Physiological Adaptations for Marine Life of
654 Salmonids: Osmoregulation, Growth, and Metabolism. Am Fish Soc Symp. 1987;1:
655 211–229.

656 49. McCarthy ID. Temporal repeatability of relative standard metabolic rate in juvenile
657 Atlantic salmon and its relation to life history variation. J Fish Biol. 2000;57: 224–238.
658 doi:10.1111/j.1095-8649.2000.tb00788.x

659 50. McCormick SD, Moyes CD, Ballantyne JS. Influence of salinity on the energetics of gill
660 and kidney of Atlantic salmon (Salmo salar). Fish Physiol Biochem. 1989;6: 243–254.
661 doi:10.1007/BF01875027

662 51. Davie A, Minghetti M, Migaud H. Seasonal Variations in Clock-Gene Expression in
663 Atlantic Salmon (Salmo salar). Chronobiol Int. 2009;26: 379–395.
664 doi:10.1080/07420520902820947

665 52. Huang T, Ruoff P, Fjelldal PG. Diurnal expression of clock genes in pineal gland and
666 brain and plasma levels of melatonin and cortisol in Atalantic salmon parr and smolts.
667 Chronobiol Int. 2010;27: 1697–1714. doi:10.3109/07420528.2010.514630

668 53. Huang T, Ruoff P, Fjelldal PG. Effect of continuous light on daily levels of plasma
669 melatonin and cortisol and expression of clock genes in the pineal gland, brain, and
670 liver in Atalantic salmon postsmolts. Chronobiol Int. 2010;27: 1715–1734.
671 doi:10.3109/07420528.2010.521272

672 54. Davies WIL, Tamai TK, Zheng L, Fu JK, Rihel J, Foster RG, et al. An extended family of
673 novel vertebrate photopigments is widely expressed and displays a diversity of
674 function. Genome Res. 2015;25: 1666–1679. doi:10.1101/gr.189886.115

675 55. Pagano C, Siauciunaite R, Idda ML, Ruggiero G, Ceinos RM, Pagano M, et al. Evolution
676 shapes the responsiveness of the D-box enhancer element to light and reactive
677 oxygen species in vertebrates. Sci Rep. 2018;8: 13180. doi:10.1038/s41598-018-
678 31570-8

679 56. Gavriouchkina D, Fischer S, Ivacevic T, Stolte J, Benes V, Dekens MPS. Thyrotroph
680 Embryonic Factor Regulates Light-Induced Transcription of Repair Genes in Zebrafish
681 Embryonic Cells. Riley BB, editor. PLoS One. 2010;5: e12542.
682 doi:10.1371/journal.pone.0012542

683 57. Wendelaar Bonga SE. The stress response in fish. Physiol Rev. 1997;77: 591–625.
684 doi:10.1152/physrev.1997.77.3.591

685 58. Isorna E, Pedro N De, Valenciano AI, Alonso-gómez ÁL. Interplay between the
686 endocrine and circadian systems in fishes. 2017. doi:10.1530/JOE-16-0330

687 59. Mommsen TP, Vijayan MM, Moon TW. Cortisol in teleosts: dynamics, mechanisms of
688 action, and metabolic regulation. Rev Fish Biol Fish. 1999;9: 211–268.

689 60. Liu C, Hu J, Qu C, Wang L, Huang G, Niu P, et al. Molecular evolution and functional
690 divergence of zebrafish (Danio rerio) cryptochrome genes. Sci Rep. 2015;5: 8113.
691 doi:10.1038/srep08113

692 61. Emms DM, Kelly S. OrthoFinder: solving fundamental biases in whole genome
693 comparisons dramatically improves orthogroup inference accuracy. Genome Biol.
694 2015; 1–14. doi:10.1186/s13059-015-0721-2

695

Acknowledgements

The authors thank all of the animal staff at Kårvik havbruksstasjonen for their expert care of their research animals. The work was supported by grants from the Tromsø forskningsstiftelse (TFS) starter grant TFS2016SW, awarded to SHW. ACW is supported by the Tromsø forskningsstiftelse (TFS) grant awarded to DGH (TFS2016DH). Research council of Norway grant number 241016 awarded to DGH. The publication charges for this article have been funded by a grant from the publication fund of UiT-The Arctic University of Norway.

Author contributions

ACW – conceived and designed the circadian and *in-vitro* experiments, collected samples, performed RNA preparation, gill culture, qPCR, bioinformatics analysis, analysed/interpreted data, prepared the manuscript and figures. **MI–** Bioinformatic analysis, osmolality measurements, data analysis and reviewed manuscript. **EHJ –** collected samples, designed and conducted the smoltification experiment, and reviewed the manuscript. **SS –** Conducted the evolutionary analysis of clock genes and revised the manuscript. **DGH** - collected samples, analysed/interpreted data, designed and conducted the smoltification experiment, and revised the manuscript. **SHW–** conceived and designed the circadian and *in-vitro* experiments, collected samples, performed RNA preparation, gill culture, analysed/interpreted data, and prepared the manuscript.

715 **Figure legends**

716 **Figure 1. Clock gene Ss4R duplicate pairs are divergently expressed in different tissues.**

717 A. Phylogenetic tree highlighting WGD events and evolution of anadromy. All species
718 represented (excluding the lamprey, ground sharks and coelacanth) were included in the
719 phylogenetic identification of Atlantic salmon clock genes. B. The mammalian molecular
720 clock network. C. Circos plot representing the Atalantic salmon chromosomes and the large
721 collinear blocks of the genome that are duplicated (grey blocks/lines). Overlayed are the
722 chromosomal positions of all Ss4R clock ohnologues, duplicated clock genes are connected
723 by a coloured line. The colour of this line represents the different orthogroups. Around the
724 outside of the circos plot sequence similarity of the loci in a 1mb window is shown as a
725 coloured bar; high similarity >95% (red), medium 95-90% (blue), low ~87% (green). Sequence
726 similarity on a genome wide level relates to approximate rediploidization time of Atlantic
727 salmon chromosomes (see grey box). D. Differential regulation of Ss4R pairs in a panel of 11
728 different tissues. For each Ss4R pair, in each tissue, an expression divergence index (EDI)
729 index was calculated (EDI= abs(log2[Gene1/Gene2)]. The graph shows a violin plot of the
730 distribution of EDI values across all tissues. The vertical black bar represents the median
731 value. Approximate rediploidisation time of the loci each pair is found on is represented by a
732 colour: red – late, blue – mid, green – early.

733 **Figure 2. The molecular clock network regulation in the Atlantic salmon.**

734 A. Diel and circadian regulation experiment design, arrows indicate tissue collection points.
735 Fish were maintained in a light dark cycle ("Diel" - short photoperiod 6 hours light: 18 dark)
736 transitioning onto either constant light (LL) or constant dark (DD). Sampling in diel conditions
737 was at a 4h resolution starting from 5 hours after lights on (Zeitgeber time - ZT5) for 24

738 hours. The green line represents the time-points used in the statistical analyses of diel
739 rhythmicity. Constant conditions are defined by circadian time (CT) which is relative to lights
740 on in the preceding cycle. The assessment of DD or LL rhythmicity was made using samples
741 from CT9 to CT29, indicated by the red and blue lines. N = 3 for all time-points.

742 B. Heatmap displays all diel rhythmic genes in OT, SV and gill. Overlap between tissues is
743 shown in the venn diagram. C. Peak-phase aligned LL and DD rhythmic genes in the OT.
744 Shaded area shows 95% confidence limit. D. Example duplicate comparisons from OT, SV and
745 gill. JKTcycle (adjP<0.05*, adjP<0.01**, adjP<0.001***, adjP<0.0001****).

746 **Figure 3. The molecular clock network shows ohnologue specific differences during a**
747 **photoperiodically driven developmental transistion.**

748 A. Photoperiodic gene expression experiment design. LL – constant light, SP – short
749 photoperiod. Time-points for sampling (n=6) indicated by arrow, sampling was conducted
750 once per time-point in mid-light phase, time scale shown is experimental days. B. Expression
751 heatmap of significantly photoperiodic (FDR<0.01) clock genes in the gill. Significant genes
752 cluster into five distinct expression patterns. Individual profiles are represented. Shaded area
753 shows 95% confidence limit where applicable. C. RNAseq counts per million profiles for
754 divergently regulated ohnologue pairs.

755 **Figure 4. Stress response implicates glucocorticoid receptor signaling in clock ohnologue**
756 **regulation.** A. Diel and circadian profile of plasma cortisol (n=4). Time axis is given in
757 continuous hours since the start of the experiment, therefore 1 to 21 represent zeitgeber
758 time (ZT) and 25 onwards is equivalent to circadian time (CT)1 to CT29. Due to the sampling
759 protocol time-points 1 and 5 are replotted from time-points 25 and 29. B. Sea-water stress
760 experiment design. LL – constant light, SP – short photoperiod, SW- sea-water challenge. C.

761 Plasma cortisol concentration in blood plasma in sea-water stress experiment (n=11-12). D.
762 Sea-water stress regulation of clock genes (n=6). Significantly regulated transcripts
763 (FDR<0.01) are shown in red. FC – fold change. E. Differential sea-water stress regulation of
764 ohnologue pairs. Significantly different pairs (Analysis of genes where one or both genes are
765 significantly regulated by seawater (FDR<0.01), then submitted to a two-way ANOVA, with
766 sea-water regulation and interaction, p<0.05) are shown in red. F. Predicted transcription
767 factor promoter binding analysis. Both sea-water induced and not-induced gene cohorts
768 were analysed. 50 motifs were specific to the sea-water induced cohort. The top four motifs
769 in each group are displayed.

770 **Figure 5: In-vitro validation of glucocorticoid stimulated clock ohnologue expression**

771 A. Dexamethasone-dependent transcript regulation experimental design. After photoperiod
772 manipulation whole gill arches (n=4) were removed and treated for 24h with glucocorticoid
773 receptor agonist dexamethasone (DEX), or dimethlysulphoxide (DMSO; control). B.
774 Comparative regulation of Cry3-Ch12/22 taken from *in vivo* sea-water stress experiment and
775 *in vitro* dexamethasone treatment. C. As in B for Nr1d2-Ch2/5 & Nr1d2-Ch14/27. D. As in B
776 for Tef-Ch1/28 & Tef-Ch3/6. Braches indicate phylogenetic relationship between gene sets.

777 **S1 Figure: Tissue specific expression of clock ohnologues**

778 A. PCA plot showing the relative tissue differences when considering clock ohnologue
779 expression. B. Heatmap showing the tissue specific expression of clock ohnologues.

780 **S2 Figure: Nanostring clock gene expression and circadian phase aligned plots**

781 A. Heatmap showing the mesor expression for each clock ohnologue in three tissues. Grey
782 indicates the gene is not expressed. B. Phase aligned plots for the gill. C. Phase aligned plot

783 for the SV. D. Arntl1-Ch10/16 comparison: plot of non-linear regression using a sixth-order
784 centered polynomial to fit the data and compare individual curves. P-value is the result of
785 extra sum-of-squares F test. E. As above for Cry3-Ch12/22.

786 **S3 Figure: Osmoregulatory capacity during the smoltification experiment**

787 A. Osmolality (mOsm kg-1) is displayed for fish in freshwater (FW – blue) and seawater (SW –
788 green) (n=6). This plot show osmoregulatory capacity develops by the two latest timepoints
789 (T5 and T6).

790 **S4 Figure: Gene expression of Tsc22d3-Ch3, a positive control gene for DEX treatment**

791 A. Gene expression of Tsc22dd3-Ch3 *in vivo* sea-water stress experiment (RNAseq counts per
792 million (cpm)) and B. *in vitro* dexamethasone treatment (qPCR).

793 **S1 Table: Clock genes identified in Atlantic Salmon, orthogroups, duplicates, significances**
794 **for the circadian, smoltification and seawater challenge experiments**

795 **S2 Table: Nanostring codeset design and qPCR primers**

796 **S3 Table: Summary of previous studies measuring cortisol in fish**

797 **S4 Table: Cortisol source data for Figure 4A**

798 **S5 Table: SalmotifDB results – transcription factor binding site analysis**

799 **S6 Table: qPCR source data for Figure5**

800 **S1 appendix: Evolutionary gene trees for circadian clock genes**

801 **S2 appendix: Nanostring circadian profiles for all genes**

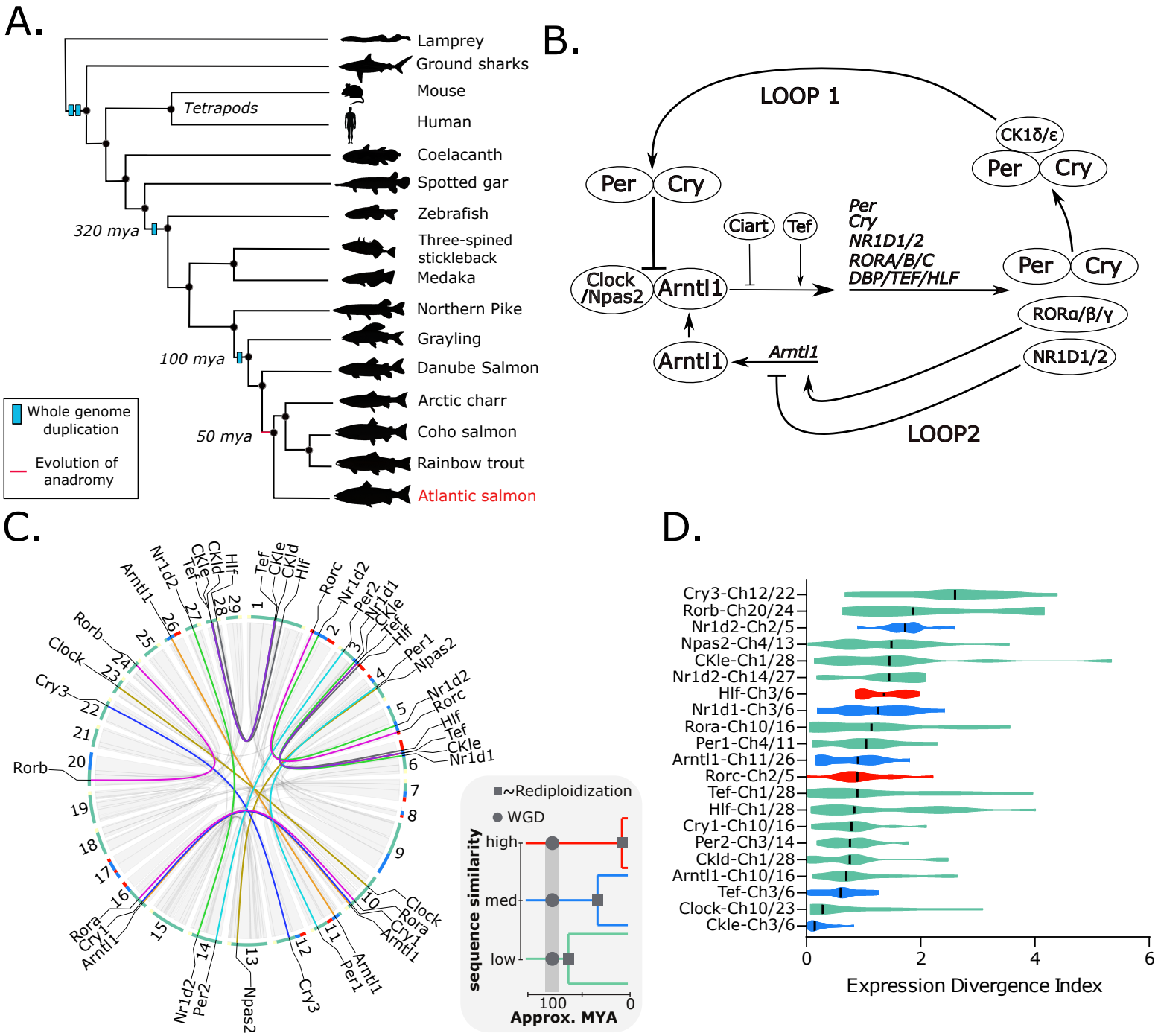
A.
Lamprey
Ground sharks
Mouse
Human
Tetrapods
Coelacanth
Spotted gar
Zebrafish
320 mya
Three-spined stickleback
Medaka
Northern Pike
Grayling
100 mya
Danube Salmon
Arctic charr
50 mya
Coho salmon
Rainbow trout
Atlantic salmon
Whole genome duplication
Evolution of anadromy
B.
LOOP 1
CK1δ/ε
Per
Cry
Per
Cry
Ciart
Tef
Per
Cry
NR1D1/2
RORA/B/C
DBP/TEF/HLF
Clock /Npas2
Arntl1
Per
Cry
RORα/β/γ
Arntl1
Arntl1
NR1D1/2
LOOP2
C.
Rorb
Clock
Cry3
Rorb
Rora
Cry1
Arntl1
Nr1d2
Per2
Npas2
Cry3
Per1
Arntl1
Clock
Rora
Cry1
Arntl1
~Rediploidization
WGD
sequence similarity
high
med
low
100
0
Approx. MYA
D.
Cry3-Ch12/22
Rorb-Ch20/24
Nr1d2-Ch2/5
Npas2-Ch4/13
CKle-Ch1/28
Nr1d2-Ch14/27
Hlf-Ch3/6
Nr1d1-Ch3/6
Rora-Ch10/16
Per1-Ch4/11
Arntl1-Ch11/26
Rorc-Ch2/5
Tef-Ch1/28
Hlf-Ch1/28
Cry1-Ch10/16
Per2-Ch3/14
Ckld-Ch1/28
Arntl1-Ch10/16
Tef-Ch3/6
Clock-Ch10/23
Ckle-Ch3/6
0
2
4
6
Expression Divergence Index

Fig. 1

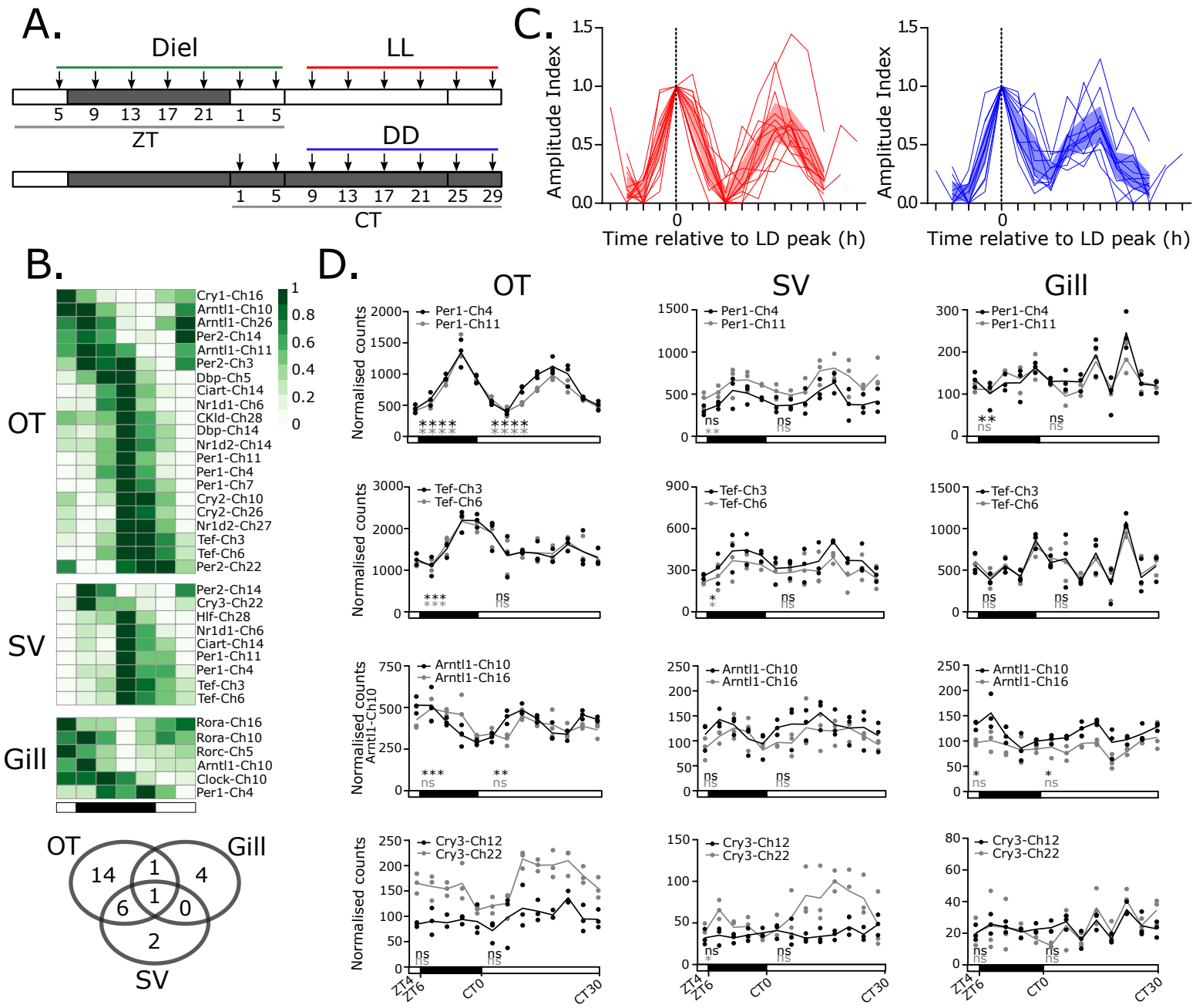
A.
Diel
LL
5 9 13 17 21 1 5
ZT
DD
1 5 9 13 17 21 25 29
CT
C.
Amplitude Index
Time relative to LD peak (h)
B.
OT
SV
Gill
Cry1-Ch16
Arntl1-Ch10
Arntl1-Ch26
Per2-Ch14
Arntl1-Ch11
Per2-Ch3
Dbp-Ch5
Ciart-Ch14
Nr1d1-Ch6
CKld-Ch28
Dbp-Ch14
Nr1d2-Ch14
Per1-Ch11
Per1-Ch4
Per1-Ch7
Cry2-Ch10
Cry2-Ch26
Nr1d2-Ch27
Tef-Ch3
Tef-Ch6
Per2-Ch22
Per2-Ch14
Cry3-Ch22
Hlf-Ch28
Nr1d1-Ch6
Ciart-Ch14
Per1-Ch11
Per1-Ch4
Tef-Ch3
Tef-Ch6
Rora-Ch16
Rora-Ch10
Rorc-Ch5
Arntl1-Ch10
Clock-Ch10
Per1-Ch4
14
1
4
1
6
0
2
D.
OT
SV
Gill
Normalised counts
Per1-Ch4
Per1-Ch11
Tef-Ch3
Tef-Ch6
Arntl1-Ch10
Arntl1-Ch16
Cry3-Ch12
Cry3-Ch22
ZT4
ZT6
CT0
CT30

Fig. 2

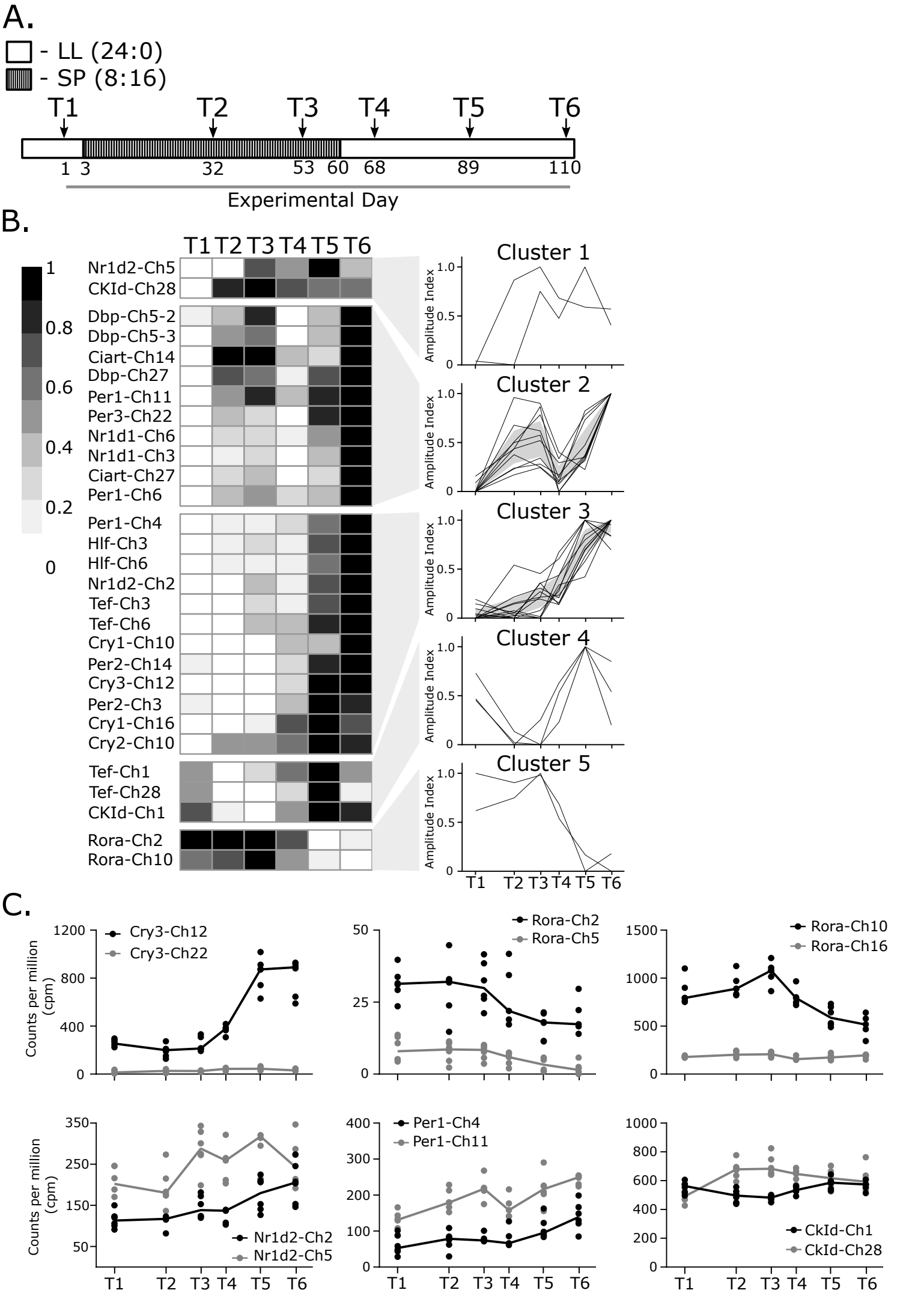
A.
- LL (24:0)
- SP (8:16)
T1
T2
T3
T4
T5
T6
1 3
32
53 60 68
89
110
Experimental Day
B.
T1 T2 T3 T4 T5 T6
1
0.8
0.6
0.4
0.2
0
Nr1d2-Ch5
CKId-Ch28
Dbp-Ch5-2
Dbp-Ch5-3
Ciart-Ch14
Dbp-Ch27
Per1-Ch11
Per3-Ch22
Nr1d1-Ch6
Nr1d1-Ch3
Ciart-Ch27
Per1-Ch6
Per1-Ch4
Hlf-Ch3
Hlf-Ch6
Nr1d2-Ch2
Tef-Ch3
Tef-Ch6
Cry1-Ch10
Per2-Ch14
Cry3-Ch12
Per2-Ch3
Cry1-Ch16
Cry2-Ch10
Tef-Ch1
Tef-Ch28
CKId-Ch1
Rora-Ch2
Rora-Ch10
Cluster 1
Cluster 2
Cluster 3
Cluster 4
Cluster 5
Amplitude Index
1.0
0.5
0
T1 T2 T3 T4 T5 T6
C.
Cry3-Ch12
Cry3-Ch22
Counts per million (cpm)
1200
800
400
0
Rora-Ch2
Rora-Ch5
50
25
0
Rora-Ch10
Rora-Ch16
1500
1000
500
0
Nr1d2-Ch2
Nr1d2-Ch5
350
250
150
50
Per1-Ch4
Per1-Ch11
400
300
200
100
0
CkId-Ch1
CkId-Ch28
1000
800
600
400
200
0
T1 T2 T3 T4 T5 T6

Fig. 3

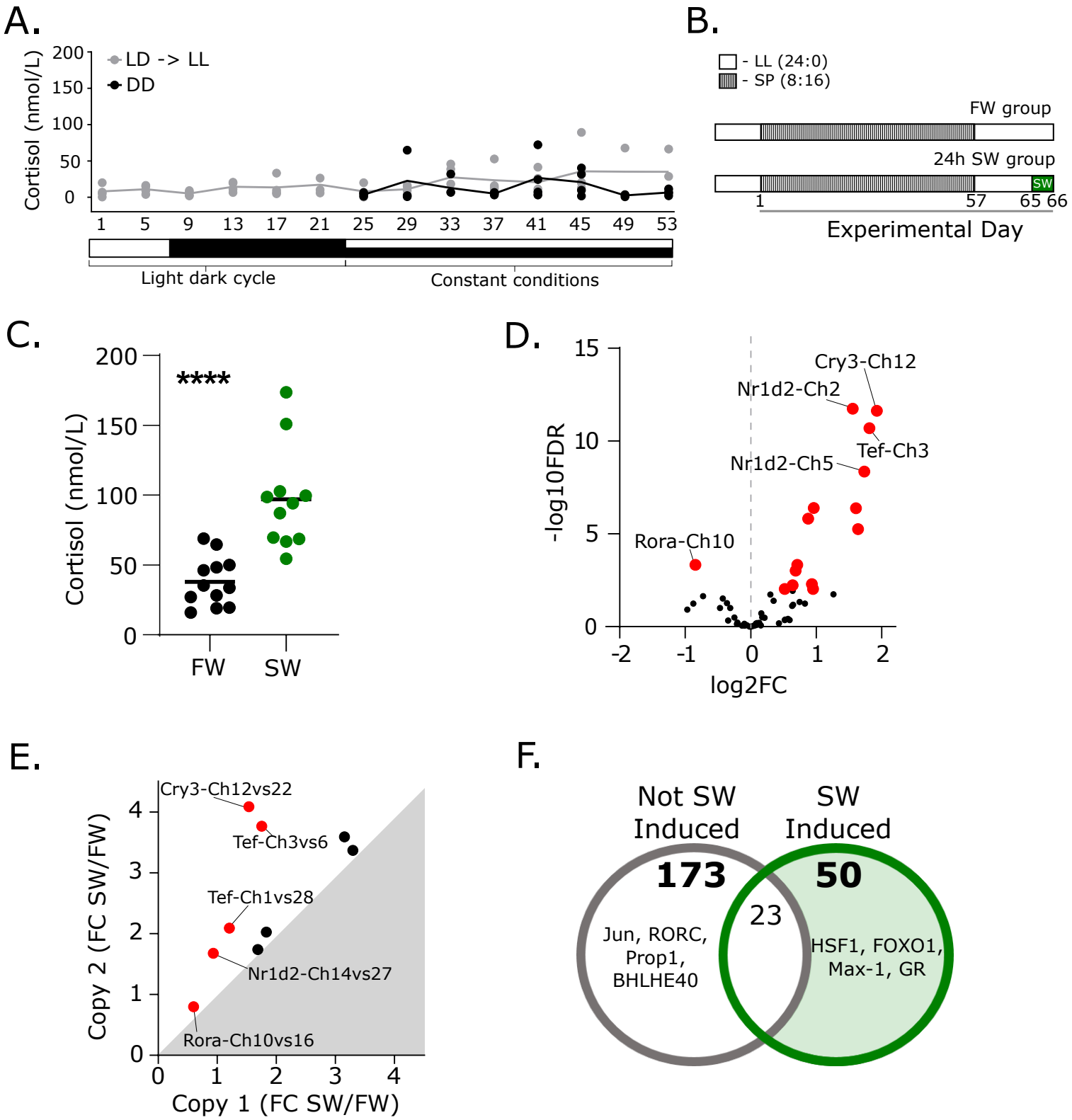
A.
Cortisol (nmol/L)
LD -> LL
DD
Light dark cycle
Constant conditions
B.
- LL (24:0)
- SP (8:16)
FW group
24h SW group
SW
Experimental Day
C.
****
Cortisol (nmol/L)
FW
SW
D.
-log10FDR
log2FC
Cry3-Ch12
Nr1d2-Ch2
Tef-Ch3
Nr1d2-Ch5
Rora-Ch10
E.
Copy 2 (FC SW/FW)
Copy 1 (FC SW/FW)
Cry3-Ch12vs22
Tef-Ch3vs6
Tef-Ch1vs28
Nr1d2-Ch14vs27
Rora-Ch10vs16
F.
Not SW Induced
SW Induced
173
50
23
Jun, RORC, Prop1, BHLHE40
HSF1, FOXO1, Max-1, GR

Fig. 4

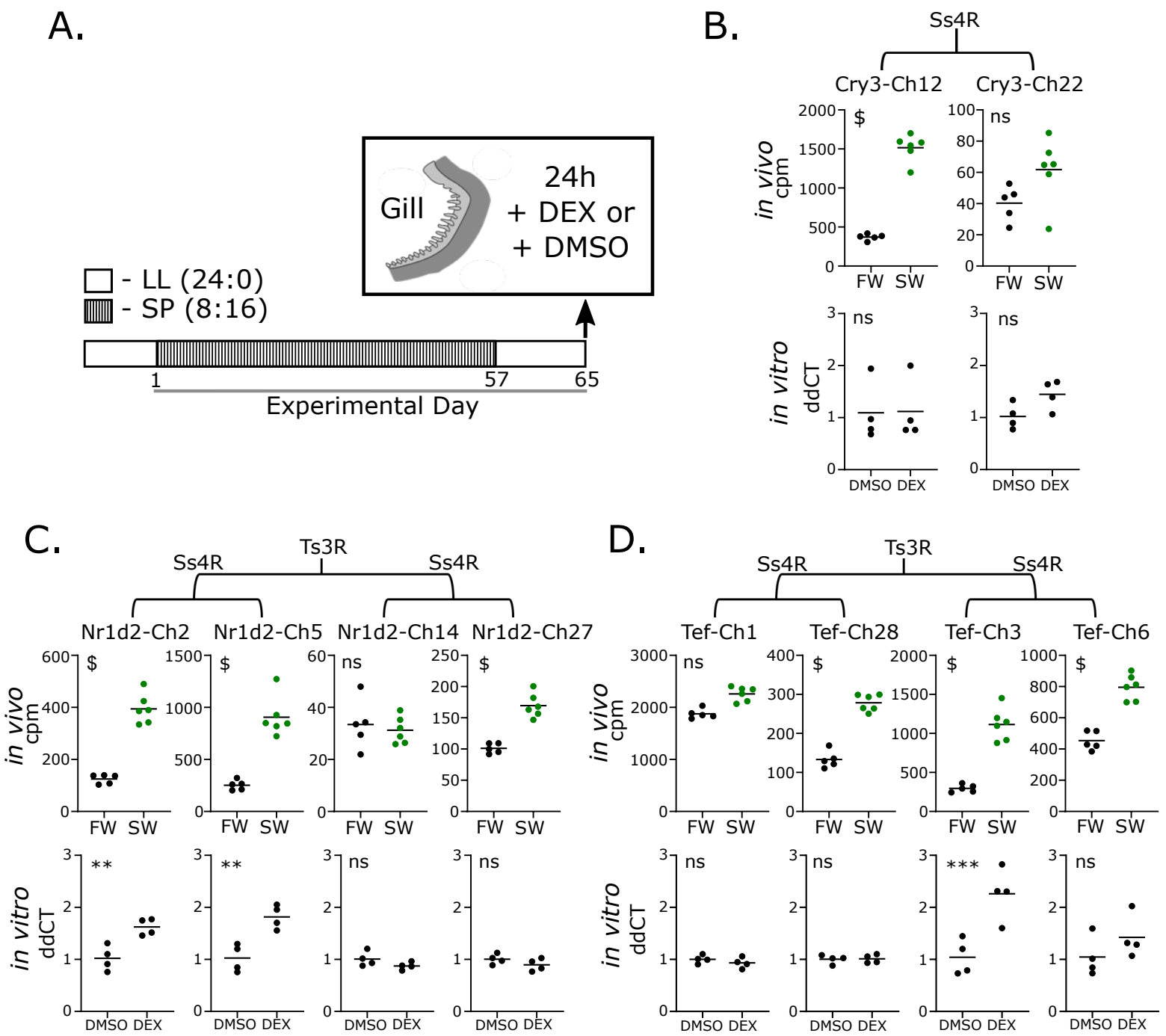
A.
Gill
24h
+ DEX or
+ DMSO
- LL (24:0)
- SP (8:16)
1
57
65
Experimental Day
B.
Ss4R
Cry3-Ch12
Cry3-Ch22
in vivo
cpm
in vitro
ddCT
FW
SW
DMSO
DEX
C.
Ss4R
Ts3R
Ss4R
Nr1d2-Ch2
Nr1d2-Ch5
Nr1d2-Ch14
Nr1d2-Ch27
D.
Ss4R
Ts3R
Ss4R
Tef-Ch1
Tef-Ch28
Tef-Ch3
Tef-Ch6

Fig. 5

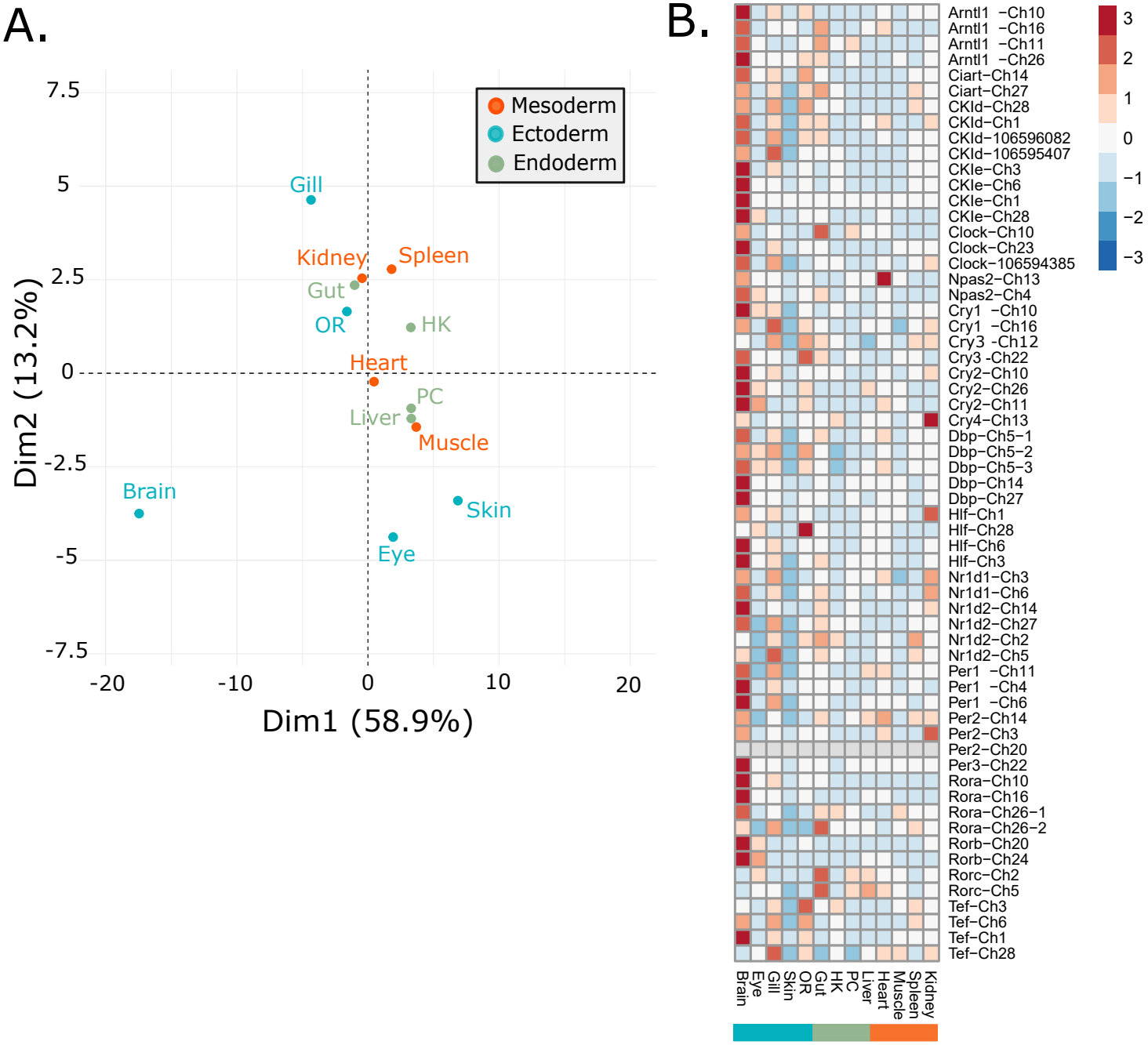

Supplementary Fig. 1

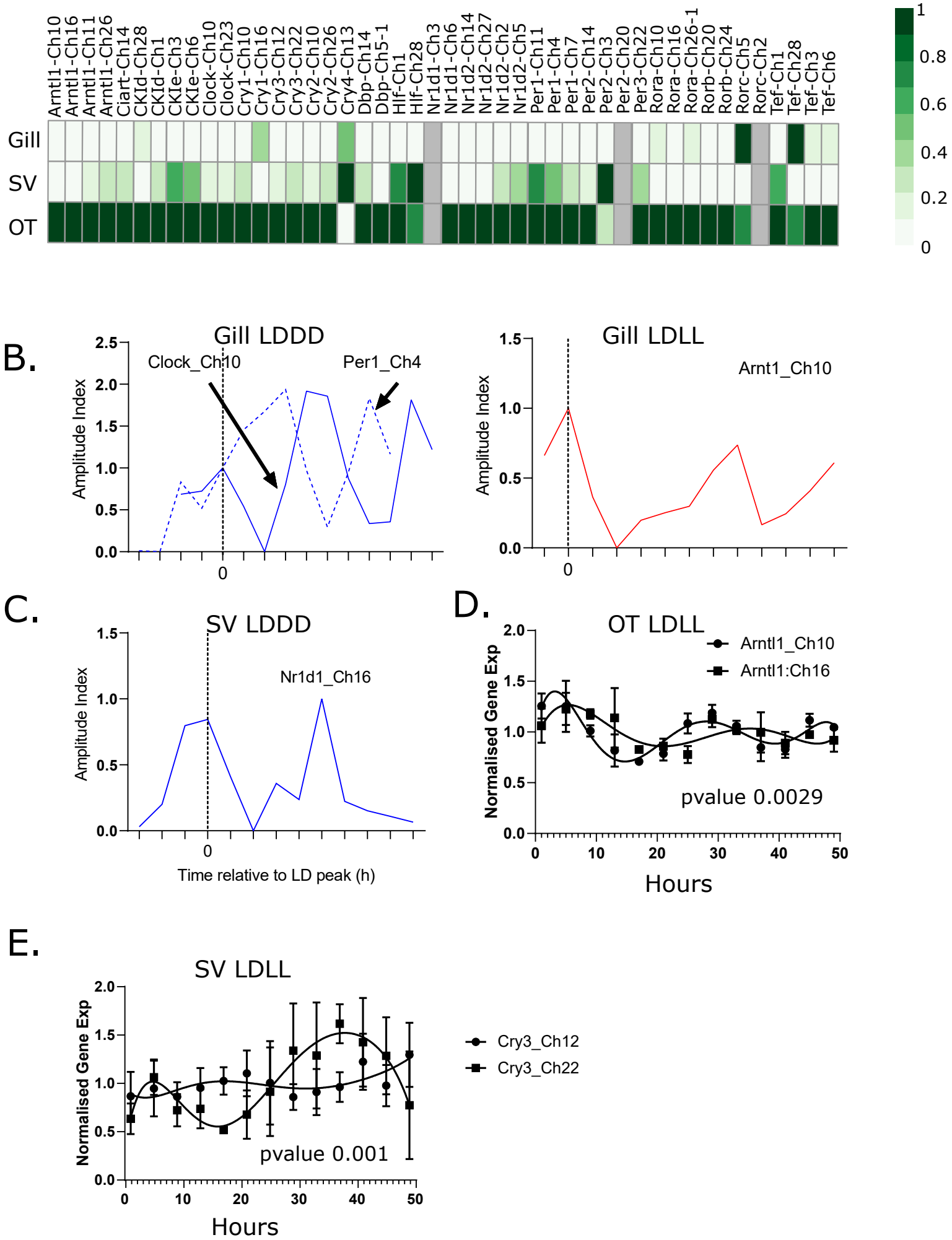

Supplementary Fig. 2

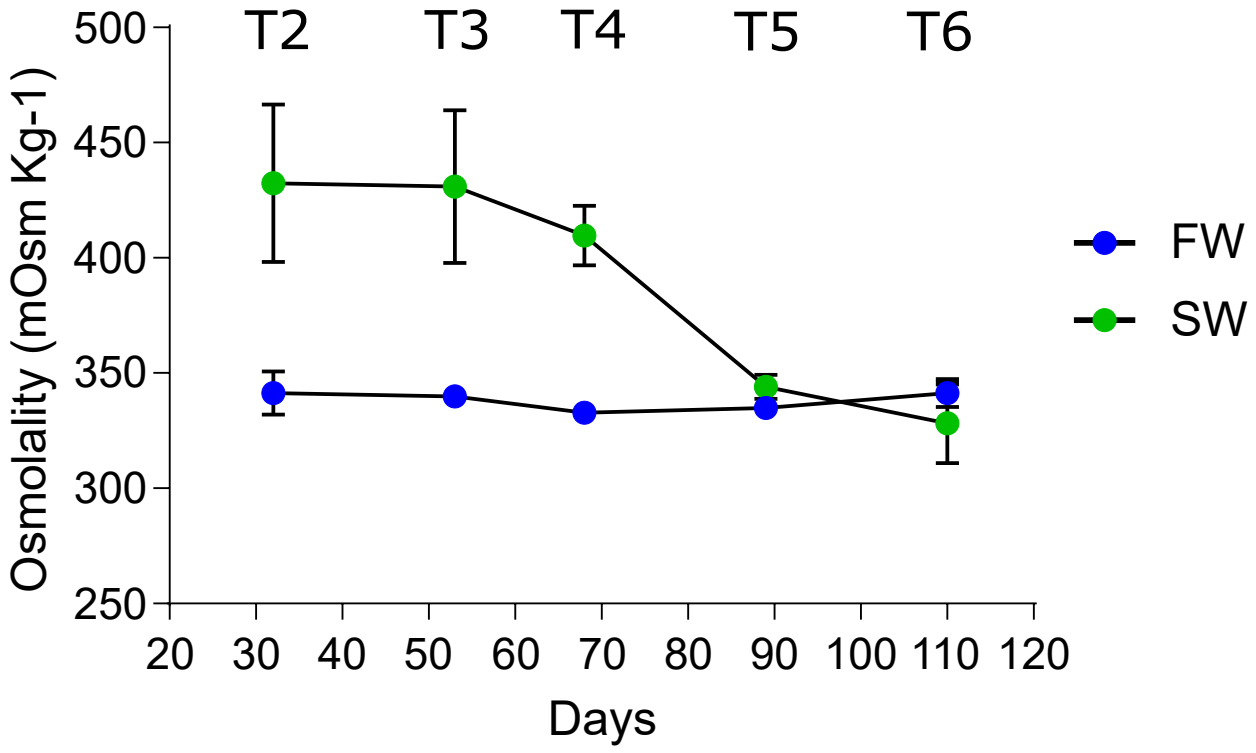

Supplementary Fig. 3

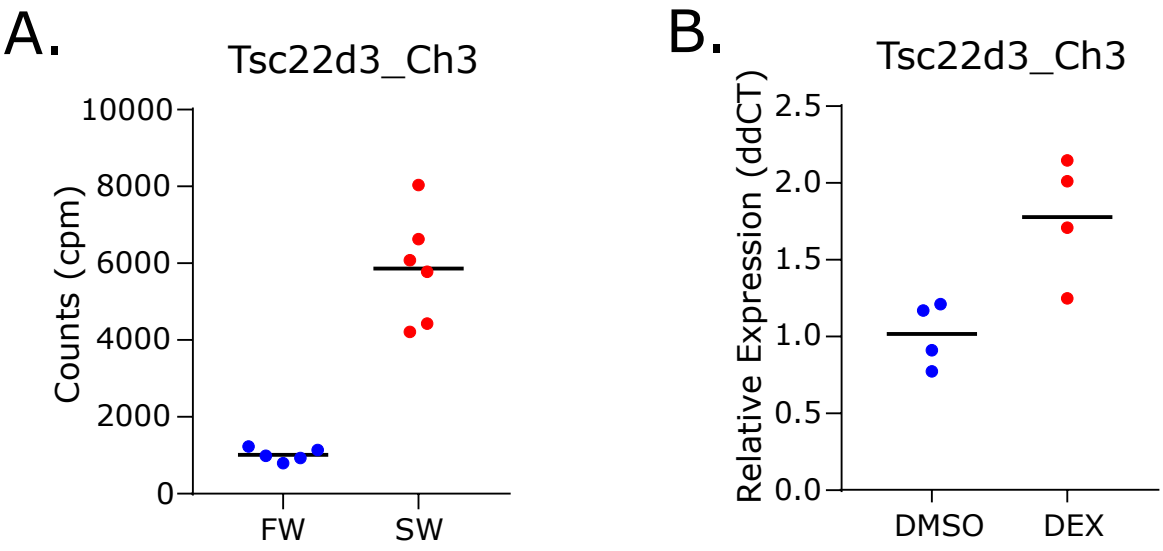

Supplementary Fig. 4